ORIGINAL ARTICLE

Quantification of the solvent evaporation rate during the production of three PVDF crystalline structure types by solvent casting

Hideo Horibe, Yasutaka Sasaki, Hironori Oshiro, Yukari Hosokawa, Akihiko Kono, Seiji Takahashi and Takashi Nishiyama

In this study, we quantified the solvent evaporation rate in the production of three poly(vinylidene fluoride) (PVDF) crystalline structures using the solvent casting method, the first known report on such quantification. The evaporation conditions of drying temperature and pressure for the solvent species during solvent casting were varied. The results indicated that the crystalline structures of forms I, II and III of PVDF were obtained when the solvent evaporation rates were <0.0001, >0.2 and between 0.03 and 0.00058 g min^{-1}, respectively. From the above quantitative analysis, it was established that the crystalline structure of PVDF from solvent casting is predominantly determined by the solvent evaporation rate.

INTRODUCTION

Poly(vinylidene fluoride) (PVDF) has three different crystalline structure types.[1–3] The crystalline structure of PVDF (form I) is plane zigzag (TTTT) while that of PVDF (form II) is twist (TGTG'). The structure of PVDF (form III) is a combination of the PVDF (form I) and PVDF (form II) structures (TTTGTTTG'), as shown in Figure 1.

PVDF (form I) possesses superior electrical characteristics such as piezoelectricity and pyroelectricity, which are caused by orientation polarization between hydrogen $(\delta+)$ and fluorine $(\delta-)$ atoms.[4] The intramolecular interaction energy of PVDF (form I) is -0.48 kcal mol^{-1} molecular unit (m.u.), while that of PVDF (form II) is -1.46 kcal mol^{-1} m.u. Furthermore, the intermolecular interaction energy of PVDF (form I) is -5.25 kcal mol^{-1} m.u., while that of PVDF (form II) is -4.57 kcal mol^{-1} m.u. Based on these data, the total potential energy of PVDF (form I) is -5.73 kcal mol^{-1} m.u., and that of PVDF (form II) is -6.03 kcal mol^{-1} m.u. Therefore, PVDF (form II) is generally more stable than PVDF (form I).[2] Many researchers have tried to control the crystalline structures of PVDF, and such control has been reported for the production of PVDF (form 1).[5–8] As a production method for PVDF (form I), we melt-blended PVDF and poly(methyl methacrylate) in a blend ratio of 70:30 wt% at 200 °C, and PVDF (form I) was obtained by quenching after sample blending.[9–14]

The three PVDF crystalline structures may be separately produced by solvent casting, which is a well-known production method of

PVDF crystalline structures with different solvents. Specifically, hexamethylphosphoramide (HMPA), acetone and dimethylacetamide (DMAc) are utilized in solvent casting for the production of PVDF (form I), PVDF (form II) and PVDF (form III), respectively. Herein, we focused on the difference in solvent boiling points (BPs). The solvent BPs of HMPA, acetone and DMAc are 233, 166 and 56 °C, respectively. Therefore, we assumed that the PVDF crystalline structures are affected by the solvent evaporation rate rather than kinds of solvent.

Based on these assumptions, we produced the three crystalline structures of PVDF using only HMPA by controlling the solvent evaporation rates.[15] PVDF (form I), PVDF (form II) and PVDF (form III) were obtained by evaporating HMPA solvent from 25 to 40 °C, from 160 to 170 °C and from 80 to 120 °C, respectively.[6] The pressure while evaporating was also changed to control the crystalline structures of PVDF. Thus, at 25 °C, PVDF (form I) and PVDF (form III) were obtained at 0.08 and 0.01 MPa, respectively, while PVDF (form II) was obtained at a pressure lower than those of the other crystalline structures.[15] We strongly believed that the crystalline structure of PVDF was heavily dependent on the solvent evaporation rate during solvent casting. Generally, the PVDF crystalline structures have kinetic advantages in the following order: PVDF (form II), PVDF (form III) and PVDF (form I). However, they have thermodynamic advantages in the reverse order.[2] The balance of kinetic and thermodynamic advantages to produce PVDF crystalline structures is easily disrupted by only a few condition variations.
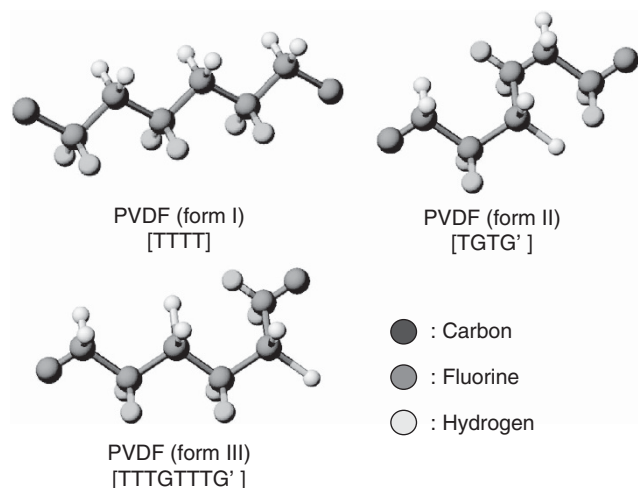
Figure 1 Three PVDF crystalline structure types.

Therefore, we can assume that the PVDF crystalline structure also undergoes a change under each condition. To our knowledge, no study has focused on the quantification of solvent evaporation rate after spin coating or the relationship between PVDF crystalline structure and solvent evaporation rate.

In this study, the solvent evaporation rate was quantified by measuring the sample weight alteration with respect to solvent evaporation time. The variation of crystalline structure was also examined by measuring the X-ray diffraction (XRD) and Fourier transform infrared (FT-IR) spectra of PVDF produced under each solvent evaporation condition. Accordingly, the relationship between solvent evaporation rate and PVDF crystalline structure was investigated.

EXPERIMENTAL PROCEDURE
Materials and reagents
In this study, PVDF powder (KUREHA Co., Tokyo, Japan, KF polymer #1100) was used. HMPA (Sigma-Aldrich, St Louis, MO, USA, 99%, BP 233 °C), acetone (Wako Pure Chemical Industries, Ltd., Osaka, Japan, 98%, BP 56 °C) and DMAc (Wako Pure Chemical Industries, Ltd., 99%, BP 166 °C) were used as solvents.

Production of standard samples of each PVDF form with solvent casting using various solvents
PVDF forms I, II and III can be produced by solvent casting using HMPA, acetone and DMAc, respectively. Based on our previous research, standard samples of each PVDF crystalline structure were prepared using HMPA, acetone and DMAc under optimum conditions.[15]

Production of PVDF (form I)
PVDF powder was dissolved in HMPA at 25 °C at a concentration of 10 wt%. The solution was held for 5 min at 25 °C and coated on a Si wafer at 500 r.p.m. for 20 s using a spin coater (Active Co., Ltd., Saitama, Japan, ACT-300 A). After spin coating, the sample was dried at 25 °C.

Production of PVDF (form II)
PVDF powder was dissolved in acetone at 56 °C at a concentration of 20 wt%. The solution was held for 5 min at 56 °C and then cooled to room temperature (25 °C). The solution was coated on a Si wafer at 500 r.p.m. for 20 s using a spin coater. After spin coating, the sample was dried at 25 °C.

Production of PVDF (form III)
PVDF powder was dissolved in DMAc at 25 °C at a concentration of 10 wt%. The solution was held for 5 min at 25 °C and then coated on a Si wafer at 500 r.p.m. for 20 s using a spin coater. After spin coating, the sample was dried at 60 °C using a hot plate (Barnstead/Thermolyne Co., Dubuque, IA, USA, Dataplate PMC 720 Series).

The drying time for each sample was determined by visual observation: 1440 h for PVDF (form I), 1 min for PVDF (form II), and 2 min for PVDF (form III).

Quantification of the solvent evaporation rate in the production of PVDF forms
PVDF powder was dissolved in HMPA, acetone and DMAc solvents to produce PVDF crystalline structures. The dissolution temperature of PVDF powder was 25 °C for HMPA, 56 °C for acetone and 25 °C for DMAc. The concentration was 20 wt%, and the dissolution time was 5 min. These solutions were spin coated onto a Si wafer at 500 r.p.m. for 20 s by a spin coater (Active Co., ACT-300A). The spin-coated sample prepared with HMPA was dried for 92 160 min (1536 h) under ambient atmosphere at 25 °C, and the samples prepared with acetone were dried for 11 min. The samples prepared with HMPA were dried under ambient atmosphere at each temperature condition (80 °C for 280 min, 100 °C for 100 min and 160 °C for 15 min) using a hot plate. The samples prepared with DMAc were dried at 40 °C for 36 min and at 60 °C for 14 min with a hot plate. The samples prepared with HMPA were dried at 25 °C for 20 160 min (336 h) at 0.08 MPa, for 3660 min (61 h) at 0.05 MPa and for 1080 min (18 h) at 0.01 MPa. Reduced-pressure drying equipment connected to a rotary pump (Ulvac Kiko Inc., Saito, Japan, G-50SA) and a stainless steel vacuum desiccator (Stainless Labotech Co., Kasukabe, Japan, SV-300) were used for drying under low pressure.

The solvent evaporation rate was quantified by measuring the sample weight with an electronic balance (Denver Instrument Co., Bohemia, NY, USA, XS-210) for each evaporation condition as described below. When the drying temperature exceeded 25 °C under ambient atmosphere, the sample weight was re-measured with an electric balance after heating constantly with a hot plate. When the drying temperature was 25 °C under ambient atmosphere, the sample weight was measured in real time with the electric balance. At 25 °C and under low pressure, the sample was placed on an electric balance in the reduced-pressure drying equipment. The dry condition of samples was confirmed from the decrease in sample weight with evaporation time.

The solvent evaporation weight was calculated by deducting the dried sample weight for each drying time from the sample weight before drying. The evaporation weight was plotted against evaporation time, and the solvent evaporation rate was obtained from the slope of that curve.

### Evaluation of PVDF crystalline structures
PVDF crystalline structures of samples produced with each solvent under the various solvent evaporation conditions were evaluated by FT-IR (Shimadzu Co., Kyoto, Japan, IR Prestige) and XRD (Rigaku Co., Tokyo, Japan, Mini Flex II). Cu-Kα rays (X-ray tube voltage of 30 kV and direct current of 15 mA) were used for XRD measurements. The scanning method was θ–2θ, and the scanning rate was 2° min^{-1}.
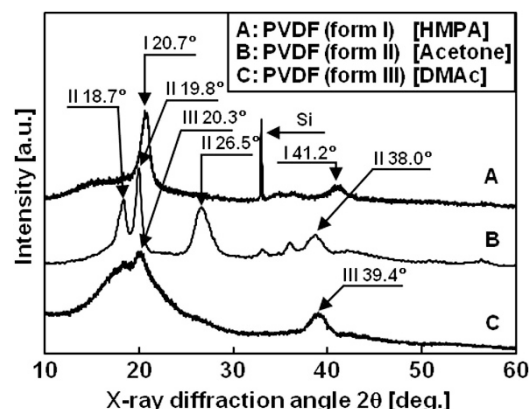
RESULTS AND DISCUSSION
Identification of PVDF crystalline structures of standard samples produced by solvent casting using HMPA, acetone and DMAc
Figure 2 shows the FT-IR spectra of standard PVDF samples produced by solvent casting using HMPA, acetone and DMAc as solvents.

In the FT-IR spectrum of the sample prepared with HMPA solvent, unique peaks of PVDF (form I) were found at 840 and 1275 cm^{-1}.[16,17] The 840 cm^{-1} peak is assigned to the CH$_2$ face angle vibration in PVDF (form I). The FT-IR spectrum of the sample produced with acetone solvent exhibited unique peaks of PVDF (form II) at 766, 795, 974 and 1210 cm^{-1}.[16,17] The 766 cm^{-1} peak is assigned to the CF stretching vibration, and the 974 cm^{-1} peak is assigned to the CH$_2$ tensional vibration in PVDF (form II). The
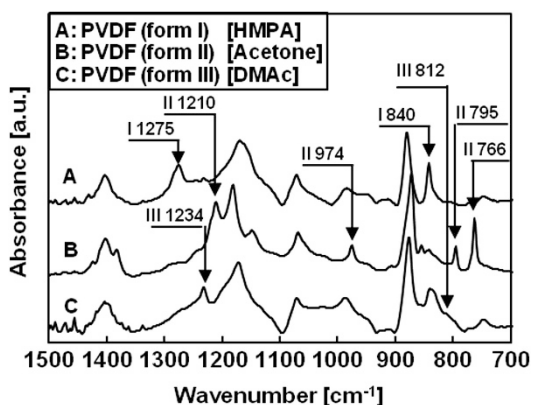
Figure 2 FT-IR spectra of standard PVDF samples produced by solvent casting using HMPA, acetone and DMAc.

Figure 3 XRD patterns of standard PVDF samples produced by solvent casting using HMPA, acetone and DMAc.

Figure 4 FT-IR spectra of PVDF samples produced by evaporating HMPA, acetone and DMAc at various drying temperatures under atmospheric conditions.

Figure 5 XRD patterns of PVDF samples produced by evaporating HMPA, acetone and DMAc at each drying temperature under atmospheric conditions.

PVDF sample produced with DMAc solvent showed unique peaks of PVDF (form III) at 812 and 1234 cm^{-1} in the FT-IR spectrum.[16,17]

Figure 3 shows the XRD patterns of the three standard PVDF crystalline structures.

From the XRD pattern of the sample prepared with HMPA solvent, peaks were observed at 20.7 and 41.2°. The peak at 20.7° corresponds to the reflective surfaces of (200) and (110). The peak at 41.2° corresponds to the reflective surfaces of (201) and (111).[18] In the XRD pattern of the sample produced with acetone solvent, peaks were observed at 18.7, 19.8, 26.5 and 38.0°, corresponding to the reflective surfaces of (020), (110), (021) and (002), respectively.[18,19] From the XRD pattern of the sample produced with DMAc solvent, peaks were observed at 20.3 and 39.4°. The peak at 20.3° corresponds to the reflective surface of (101) and that at 39.4° corresponds to (401) and (132).[20] These XRD and IR results from the standards were utilized to identify the crystalline structure of samples produced under each condition.

Identification of PVDF crystalline structures of samples produced by changing drying temperature after spin coating with various solvents
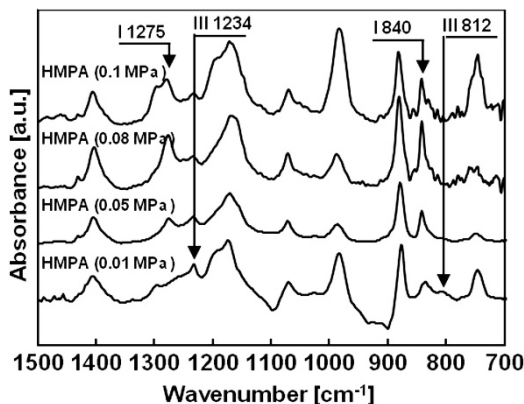
To evaluate the variation of PVDF crystalline structures according to differences in solvent evaporation rate, the crystalline structures of PVDF samples produced by changing drying temperatures and using various solvents were identified. Figure 4 shows the FT-IR spectra of PVDF samples produced by evaporating HMPA, acetone and DMAc at various drying temperatures.

In the FT-IR spectrum of the sample produced by evaporating HMPA solvent at 25 °C, unique peaks of PVDF (form I) were found at 840 and 1275 cm^{-1}. In the FT-IR spectra of samples produced by evaporating DMAc solvent at 40 and 60 °C or HMPA solvent at 80 and 100 °C, unique peaks of PVDF (form III) were found at 812 and 1234 cm^{-1}. In the FT-IR spectra of samples produced by evaporating HMPA solvent at 160 °C or by evaporating acetone solvent at 25 °C, unique peaks of PVDF (form II) were found at 766, 795, 974 and 1210 cm^{-1}.

Figure 5 shows the XRD patterns of PVDF samples produced by evaporating HMPA, acetone and DMAc at each drying temperature. In the XRD pattern of the sample produced by evaporating HMPA solvent at 25 °C, unique peaks of PVDF (form I) were confirmed at 20.7 and 41.2°. In XRD patterns of samples produced by evaporating HMPA at 80 and 100 °C and DMAc at 40 °C, unique peaks of PVDF (form III) were confirmed at 20.3 and 39.4°. In the XRD pattern of
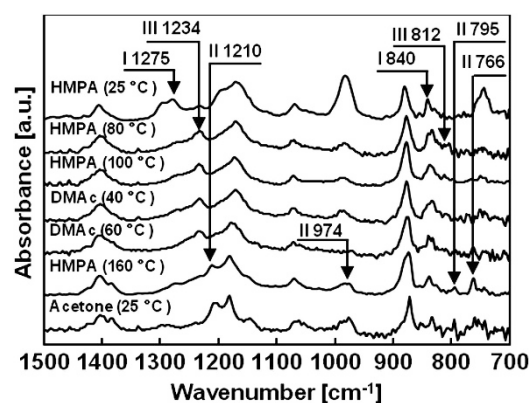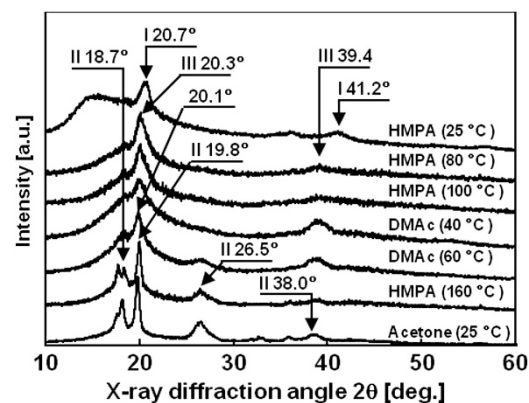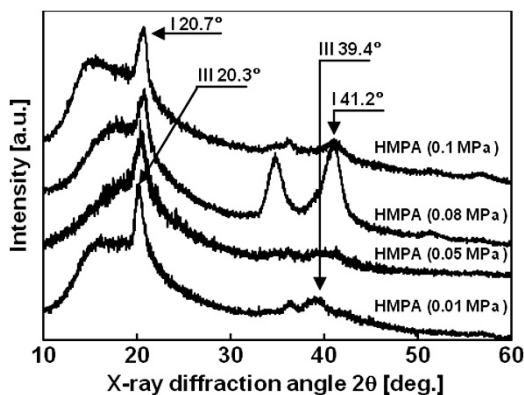
the sample produced by evaporating DMAc solvent at 60 °C, the unique peak of PVDF (form II) was confirmed at 26.5° and that of PVDF (form III) at 39.4°. A peak at 20.1° was also confirmed, which is a middle-point peak of PVDF (form III) at 20.3°. The sample of DMAc produced at 60 °C contained both PVDF (form II) and PVDF (form III). In the XRD pattern of the sample produced by evaporating

HMPA solvent at 160 °C, unique peaks of PVDF (form II) were confirmed at 18.7, 19.8 and 26.5°. In the XRD pattern of the sample produced by evaporating acetone solvent at 25 °C, unique peaks of PVDF (form II) were confirmed at 18.7, 19.8, 26.5 and 38.0°. Therefore, these samples were identified as PVDF (form II).[14]
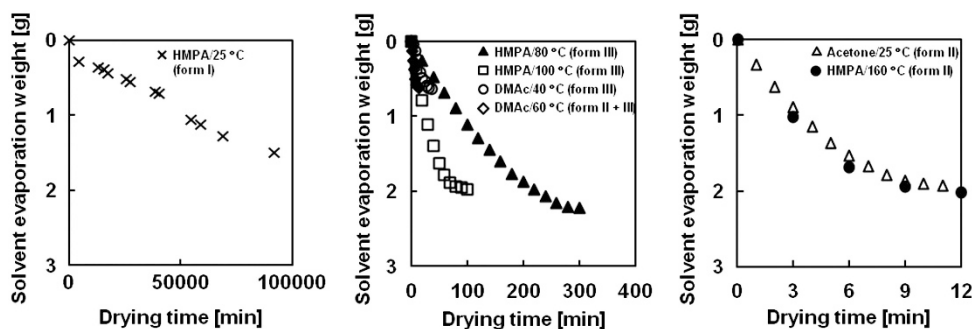
Based on the XRD and FT-IR results, the sample produced by evaporating HMPA at 25 °C was confirmed as PVDF (form I). The samples produced by evaporating HMPA at 80 and 100 °C and DMAc at 40 °C were confirmed as PVDF (form III). The sample produced by evaporating DMAc at 60 °C was PVDF (forms II + III). The samples produced by evaporating HMPA at 160 °C and acetone at 25 °C were confirmed as PVDF (form II).

Figure 6 FT-IR spectra of PVDF samples produced by evaporating HMPA solvent at 25 °C under various drying pressures.

Figure 7 XRD patterns of samples produced by evaporating HMPA solvent at 25 °C under various drying pressures.

Identification of PVDF crystalline structures of samples produced by changing only the drying pressure after spin coating with HMPA solvent

Figure 6 shows the FT-IR spectra of PVDF samples produced by evaporating HMPA solvent at 25 °C under different drying pressures. In the FT-IR spectrum of the sample produced by evaporating HMPA at 0.08 MPa, unique peaks of PVDF (form I) were found at 840 and 1275 cm^{-1}. In the FT-IR spectrum of the sample produced by evaporating HMPA at 0.05 MPa, unique peaks of PVDF (form I) were found at 840 and 1275 cm^{-1}, and unique peaks of PVDF (form III) were also found at 812 and 1234 cm^{-1}. Consequently, the sample produced by evaporating HMPA at 0.05 MPa contained both PVDF (form I) and PVDF (form III). In the FT-IR spectrum of the sample produced by evaporating HMPA at 0.01 MPa, unique peaks of PVDF (form III) were found at 812 and 1234 cm^{-1}.

Figure 7 shows the XRD patterns of samples produced by evaporating HMPA at 25 °C under different pressures.

In the XRD pattern of the sample produced by evaporating HMPA at 25 °C under 0.08 MPa, unique peaks of PVDF (form I) were confirmed at 20.7 and 41.2°. In the XRD pattern of the sample produced by evaporating HMPA at 25 °C under 0.05 MPa, a peak was found at 20.5° that was broad due to overlap of peaks at 20.7° of PVDF (form I) and 20.3° of PVDF (form III). Overlapping small peaks were found at 41.2° of PVDF (form I) and 39.4° of PVDF (form III) in the broad region from 38 to 42°. Therefore, the sample was identified as PVDF (forms I + III). In the XRD pattern of the sample produced by evaporating HMPA at 25 °C under 0.01 MPa, unique peaks of PVDF (form III) were confirmed at 20.3 and 39.4°. From these results, the samples produced by evaporating HMPA under 0.08, 0.05 and 0.01 MPa were confirmed as PVDF (form I), PVDF (forms I + III) and PVDF (form III), respectively.

Quantification of the solvent evaporation rate obtained for PVDF crystalline structures

In our previous study, we demonstrated that PVDF crystalline structures can be produced in various solvent evaporation conditions after solvent casting.[14] Even when the drying temperature and/or solvent species and only the drying pressure were varied, the three PVDF crystalline structures were obtained in the order of PVDF (II), PVDF (III) and PVDF (I) reflecting the solvent evaporation rates in increasing order. We assumed that the determination of PVDF crystalline structures was dominated by the solvent evaporation rate even under different conditions.

Based on that assumption, we attempted to quantitatively evaluate the relationship between the solvent evaporation rate at each evaporation condition and the PVDF crystalline structure. In the

Figure 8 Relationship between sample drying time and solvent evaporation weight for different solvents and/or drying temperatures.

following section, the relationship between PVDF crystalline structure and solvent evaporation rate with various solvents and/or dry temperatures is analyzed.

Quantification of solvent evaporation rate for solvent evaporation conditions with various solvents at different drying temperatures

The solvent evaporation rate was first evaluated for each condition in which a PVDF crystalline structure was obtained by using different solvents at different drying temperatures. Figure 8 shows the relationship between drying time and solvent evaporation weight for different solvents and drying temperatures. The left graph shows the relationship between sample drying time and solvent evaporation weight for PVDF (form I) with HMPA at 25 °C in an atmosphere of 0.1 MPa. The middle graph shows the relationship between sample drying time and solvent evaporation weight when PVDF (form III) and (forms II + III) were obtained. In this graph, HMPA solvent was used at 80 and 100 °C (form III) in ambient atmosphere, and DMAc solvent was used at 40 °C (form III) and 60 °C (forms II + III) in ambient atmosphere. The right graph shows the relationship between sample drying time and solvent evaporation weight when PVDF (form II) was obtained using acetone at 25 °C and HMPA at 160 °C in ambient atmosphere.

The solvent evaporation rates at each condition were calculated from the slopes of the curves in Figure 8. Each line was drawn in the most linear region from the beginning of each curve. For the sake of clarity, a line for each curve was not included in the figure. In the left graph, the solvent evaporation rate calculated for PVDF (form I) was $0.00002\,g\,min^{-1}$ using HMPA at 25 °C. For the middle graph, the solvent evaporation rates calculated for pure PVDF (form III) were $0.03\,g\,min^{-1}$ using HMPA at 100 °C, $0.02\,g\,min^{-1}$ using DMAc at

40 °C and $0.01\,g\,min^{-1}$ using HMPA at 80 °C. PVDF (forms II + III), which exhibits the binary crystalline structures of PVDF (form II) and PVDF (form III), was obtained at $0.06\,g\,min^{-1}$ using DMAc at 60 °C. As shown in the right graph, the solvent evaporation rate calculated for PVDF (form II) was $0.2\,g\,min^{-1}$ using acetone at 25 °C and HMPA at 160 °C. These results are shown in Table 1.

The solvent evaporation rate of DMAc solvent at 60 °C was $0.06\,g\,min^{-1}$, and the PVDF crystalline structure contained both PVDF (form II) and PVDF (form III).

When the solvent evaporation rate was $0.03\,g\,min^{-1}$ (slower than $0.06\,g\,min^{-1}$), the sample was pure PVDF (form III). In contrast, when the solvent evaporation rate was $0.2\,g\,min^{-1}$ (faster than $0.06\,g\,min^{-1}$), the samples were formed in PVDF (form II), and PVDF (form I) was obtained at the lowest solvent evaporation rate of $0.00002\,g\,min^{-1}$. As described above, Table 1 indicates that a region in which each PVDF crystalline structure can be obtained exists between the quantified solvent evaporation rates.

Quantification of solvent evaporation rate for different drying pressures under which PVDF crystalline structures were obtained

The solvent evaporation rates were also evaluated at conditions in which only the drying pressure was changed. Figure 9 shows the relationship between sample weight and drying time of the sample produced by evaporating HMPA solvent. The left graph shows the relationship between sample drying time and solvent evaporation weight for PVDF (form I) produced with HMPA at 25 °C and 0.08 MPa. For a comparison, the solvent evaporation curve that produced PVDF (form I) with HMPA at 25 °C in an atmosphere of 0.1 MPa is also indicated. The right graph shows the relationship between sample drying time and solvent evaporation weight for PVDF (form III) produced with HMPA at 25 °C in 0.01 MPa and PVDF (form I + III) with HMPA at 25 °C in 0.05 MPa. The solvent evaporation rates were also obtained from each curve by the same method described in the preceding section.

The solvent evaporation rate for PVDF (form I) was $0.0001\,g\,min^{-1}$ at 0.08 MPa. PVDF (form III) and PVDF (forms I + III) were obtained at solvent evaporation rates of $0.0058\,g\,min^{-1}$ at 0.01 MPa and $0.00019\,g\,min^{-1}$ at 0.05 MPa, respectively. Table 2 lists the solvent evaporation rates for each drying pressure and PVDF crystalline structure.

Table 2 indicates that PVDF (form I) and (form III) could be prepared by changing only the drying pressure with HMPA solvent at 25 °C. PVDF (form I) was obtained when the solvent evaporation rate was $<0.0001\,g\,min^{-1}$ at 0.08 MPa. PVDF (form III) was obtained when the solvent evaporation rate was $0.00058\,g\,min^{-1}$ at 0.01 MPa.

Table 1 Relationship between PVDF crystalline structure and solvent evaporation rate when changing the drying temperature and/or the solvent

Evaporation condition	Crystalline structure	Evaporation rate (g min^{-1})
HMPA/25 °C	Form I	0.00002
HMPA/80 °C	Form III	0.01
DMAc/40 °C	Form III	0.02
HMPA/100 °C	Form III	0.03
DMAc/60 °C	Forms II + III	0.06
HMPA/160 °C	Form II	0.2
Acetone/25 °C	Form II	0.2

Abbreviations: DMAc, dimethylacetamide; HMPA, hexamethylphosphoramide; PVDF, poly(vinylidene fluoride).
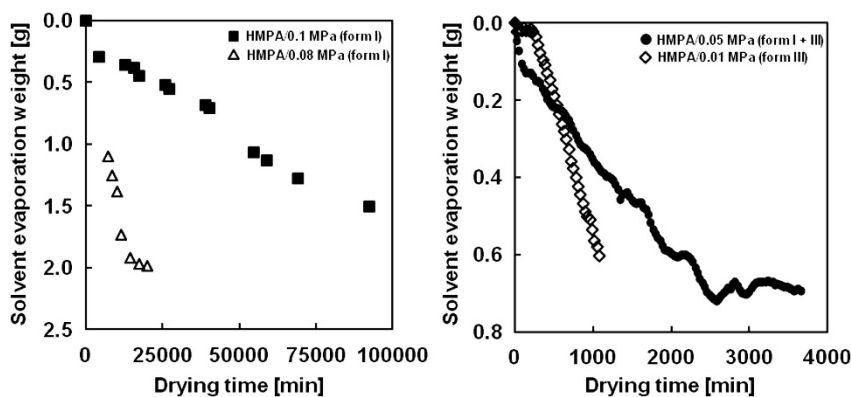
Figure 9 Relationship between sample drying time and sample evaporation weight for different drying pressures.

PVDF (form I + III) was obtained at 0.00019 g min^{-1}, which is between the rate of 0.0001 g min^{-1} obtained for PVDF (form I) and the rate of 0.00058 g min^{-1} obtained for PVDF (form III). Thus, we assume that the threshold between PVDF (form I) and PVDF (form III) is near 0.00019 g min^{-1}.

Relationship between solvent evaporation rate and PVDF crystalline structure

In our previous study, PVDF crystalline structure was controlled by changing the solvent evaporation rate for drying temperature and pressure by solvent casting. It was assumed that the solvent evaporation rate is the dominant factor in controlling the PVDF crystalline structure produced by solvent casting. In the present report, the solvent evaporation rates obtained for crystalline structures under different conditions were evaluated. If our previous assumption was correct, then we should be able to determine the relationship between PVDF crystalline structure and solvent evaporation rate obtained under different conditions. Figure 10 shows the relationship between PVDF crystalline structure and solvent evaporation rate at different evaporation conditions.

In Figure 10, the vertical axis represents the solvent evaporation rate, and the horizontal axis represents the obtained PVDF crystalline structures and evaporation conditions. The numbers in the plots indicate the solvent evaporation rates. In Figure 10, the order of the horizontal axis may not be based on scientific grounds. For each condition, we simply arranged the results in the order of solvent evaporation rate. Nevertheless, PVDF crystalline structures that corresponded to those result were ordered as PVDF (form II), (form

III) and (form I). Figure 10 is incomplete due to insufficient data. However, the regions that could be used to obtain each crystalline structure were easily confirmed. Moreover, the middle regions are found in Figure 10, in which PVDF (forms II + III) and (forms I + III) can be obtained. If the solvent evaporation rate for each region produces the crystalline structure, then the crystalline structure that corresponds with that region can be obtained regardless of the drying temperature, drying pressure or solvent species. These results supported our previous assumption that PVDF crystalline structures are predominantly determined by the solvent evaporation rate. However, these results also suggest that the interactions of solvent and temperature do not influence the determination of PVDF crystalline structure more than the solvent evaporation rate.

Through quantification of the solvent evaporation rate that produces each PVDF crystalline structure, we verified that PVDF (form II) is obtained when the solvent evaporation rate after spin coating exceeds 0.2 g min^{-1}, that PVDF (form III) is obtained when the solvent evaporation rate is between 0.00058 and 0.03 g min^{-1} and that PVDF (form I) is obtained when the solvent evaporation rate is <0.0001 g min^{-1}. Finally, the thresholds between the PVDF crystalline structures exist near 0.06 g min^{-1} (forms II + III) and 0.00019 g min^{-1} (forms I + III).

## CONCLUSIONS

In this study, the solvent evaporation rate was quantified for the production of PVDF crystalline structures by solvent casting. The relationship between PVDF crystalline structure and solvent evaporation rate was analyzed, and the solvent evaporation rate for each PVDF crystalline structure was quantified. Regardless of the evaporation conditions, the order of crystal structures was forms II, III and I, in decreasing order of solvent evaporation rate. These results support our previous assumption that PVDF crystalline structure is predominantly determined by the solvent evaporation rate. PVDF (form I) was obtained when the solvent evaporation rate was <0.0001 g min^{-1}, PVDF (form II) was obtained when the solvent evaporation rate >0.2 g min^{-1}, and PVDF (form III) was obtained when the solvent evaporation rate was between 0.00058 and 0.03 g min^{-1}.

Table 2 Relationship between PVDF crystalline structure and solvent evaporation rate when changing the drying pressure using HMPA

Evaporation condition	Crystalline structure	Evaporation rate (g min^{-1})
HMPA/25 °C (0.1 MPa)	Form I	0.00002
HMPA/25 °C (0.08 MPa)	Form I	0.0001
HMPA/25 °C (0.05 MPa)	Forms I + III	0.00019
HMPA/25 °C (0.01 MPa)	Form III	0.00058

Abbreviations: HMPA, hexamethylphosphoramide; PVDF, poly(vinylidene fluoride).
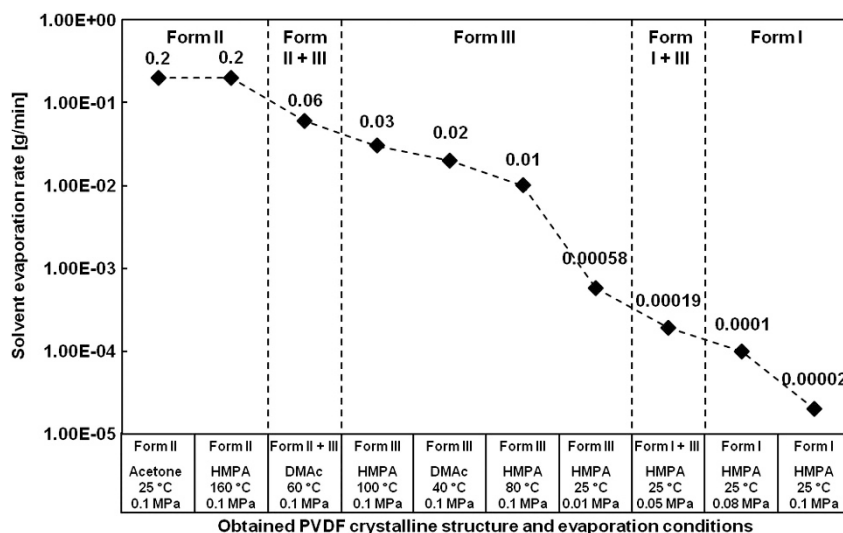
Figure 10 Relationship between PVDF crystalline structure and solvent evaporation rate for various evaporation conditions.

1 The Society of Polymer Science, Japan (ed.), *Kobunshi Bussei no Kiso,* 207, (Kyoritsu Shuppan, Tokyo, 1993) in Japanese.

2 Hasegawa, R., Kobayashi, M. & Tadokoro, H. Molecular conformation and packing of poly(vinylidene fluoride). stability of three crystalline forms and the effect of high pressure. *Polym. J.* **3,** 591–599 (1972).

3 Hasegawa, R., Takahashi, Y., Chatani, Y. & Tadokoro, H. Crystal structures of three crystalline forms of poly(vinylidene fluoride). *Polym. J.* **3,** 600–610 (1972).

4 Miyairi, K. *Denshi Bussei no Kiso,* 103, (Morikita Publishing, Tokyo, 1993) in Japanese.

5 Nasir, M., Matsumoto, H., Minagawa, M., Tanioka, A., Danno, T. & Horibe, H. Preparation of PVDF/PMMA blend nanofibers by electrospray deposition: effects of blending ratio and humidity. *Polym. J.* **41,** 402–406 (2009).

6 Danno, T., Nasir, M., Matsumoto, H., Minagawa, M., Tanioka, A. & Horibe, H. Fine structure of PVDF nanofiber fabricated by electrospray deposition. *J. Polym. Sci., Part B: Polym. Phys.* **46,** 558–563 (2008).

7 Nasir, M., Matsumoto, H., Minagawa, M., Tanioka, A., Danno, T. & Horibe, H. Preparation of porous PVDF nanofiber from PVDF/PVP blend by electrospray deposition. *Polym. J.* **39,** 1060–1064 (2007).

8 Nasir, M., Matsumoto, H., Minagawa, M., Tanioka, A., Danno, T. & Horibe, H. Formation of β-phase crystalline structure of PVDF nanofiber by electrospray deposition: additive effect of ionic fluorinated surfactant. *Polym. J.* **39,** 670–674 (2007).

9 Horibe, H. & Baba, F. Relationship between UV transmittance and poly (vinylidene fluoride) crystal structures of poly (vinylidene fluoride)/poly (methyl methacrylate) blends after annealing. *Kobunshi Ronbunsyu* **57,** 403–411 (2000) in Japanese.

10 Horibe, H. & Baba, F. Changes in crystal structures of PVDF in PVDF/PMMA blends heat-treated in several ways. *Nihon Kagakukaishi* **2,** 121–126 (2000) in Japanese.

11 Horibe, H. & Baba, F. Relationship between UV transmittance and compatibility of PVDF/PMMA blends. *Nihon Kagakukaishi* **2,** 115–120 (2000) in Japanese.

12 Horibe, H. & Taniyama, M. poly (vinylidene fluoride) crystal structure of poly (vinylidene fluoride) and poly (methyl methacrylate) blend after annealing. *J. Electrochem. Soc.* **153,** G119–G124 (2006).

13 Danno, T., Matsumoto, H., Nasir, M., Minagawa, M., Horibe, H. & Tanioka, A. PVDF/PMMA composite nanofiber fabricated by electrospray deposition: Crystallization of PVDF induced by solvent extraction of PMMA component. *J. Appl. Polym. Sci.* **112,** 1868–1872 (2009).

14 Oshiro, H., Kono, A., Danno, T. & Horibe, H. Crystal structure control of poly(vinylidene fluoride) (PVDF) in the blend films of PVDF and poly(methyl methacrylate) (PMMA) prepared by solvent casting. *Kobunshi Ronbunsyu* **69,** 135–141 (2012) in Japanese.

15 Oshiro, H., Sato, T., Yamamoto, M., Kono, A., Horibe, H., Masunaga, H., Danno, T., Matsumoto, H. & Tanioka, A. Crystal structure control of poly (vinylidene fluoride) using solvent casting. *Kobunshi Ronbunsyu* **67,** 632–639 (2010) in Japanese.

16 Bormashenko, Y., Pogreb, R., Stanevsky, O. & Bormashenko, E. d. Vibrational spectrum of PVDF and its interpretation. *Polym. Test* **23,** 791–796 (2004).

17 Kobayashi, M., Tashiro, K. & Tadokoro, H. Molecular vibrations of three crystal forms of poly(vinylidene fluoride). *Macromolecules* **8,** 158–171 (1975).

18 Matsushige, K. & Takemura, T. Melting and crystallization of poly (vinylidene fluoride) under high pressure. *J. Polym. Sci. Part B: Polym. Phys.* **16,** 921–934 (1978).

19 Yu, S., Zheng, W., Yu, W., Zhang, Y., Jiang, Q. & Zhao, Z. Formation mechanism of β-phase in PVDF/CNT composite prepared by the sonication method. *Macromolecules* **42,** 8870–8874 (2009).

20 Takahashi, Y. & Tadokoro, A. Kink bands in form I of poly (vinylidene fluoride). *Macromolecules* **13,** 1318–1320 (1980).